

Design of a Rail-gun System to Launch Cube Satellites and Other Small Payloads into Orbit

Mahbub Ahmed

2016

Design of a Rail-gun System to Launch Cube Satellites and Other Small Payloads into Orbit

MAHBUB AHMED

Contents

1	DECLARATION	5
2	INTRODUCTION	7
3	BACKGROUND	7
3.1	ELECTROMAGNETIC LAUNCHERS	7
3.2	ARMATURES	10
3.3	PROJECTILE DESIGN	11
4	CALCULATIONS	12
4.1	THE BIOT-SAVART LAW	12
4.2	MAGNETIC FIELD STRENGTH IN A RAIL GUN	15
4.3	THE LORENTZ FORCE	17
4.4	STEADY CURRENT	18
4.5	PULSED CURRENT	19
5	SIMULATIONS	23
5.1	ASSUMPTIONS AND PARAMETERS	23
5.2	MATLAB SIMULATIONS	25
6	DISCUSSION	27
7	APPENDIX	28
7.1	APPENDIX I: LORENTZ FORCE INTEGRAL DERIVATION	28
7.2	APPENDIX II: MATLAB CODE FOR SIMULATIONS	31
7.3	APPENDIX III: ANSYS SIMULATIONS	33
8	REFERENCES	35

1 DECLARATION

Queen Mary University of London

School of Engineering & Materials Science

Aerospace Engineering

DEN318

Third Year Project Technical Report

April 2016

Declaration:

This report entitled:

Design of a Rail-gun System to Launch Cube Satellites and Other Small Payloads into Orbit

was composed by me, and is based on my own work. Where work of others has been used, it has been fully acknowledged in the text and in captions to table illustrations. This report has not been submitted for any other qualification.

Name: Mahbub Ahmed

Candidate No.: 130002059

Signed:

Date:

2 INTRODUCTION

This study looks into the potential use of an electromagnetic launch system (EMLS) to launch small payloads, specifically cube satellites (also known as miniature satellites), of mass < 10 kg into low earth orbit (from which transfer manoeuvres can be used to reach higher altitudes of orbit).

Cube satellite are small satellites of dimensions $10 \times 10 \times 10 \text{ m}^3$, and are becoming more and more commonplace in the commercial, industrial and even educational sector. This is attributed to advances in microelectronics that have allowed us to incorporate full large scale satellite capabilities into a device that is no larger than the palm of your hand. Such satellites are used to conduct small scale projects such as the detection of cosmic radiation and the study of meteorological phenomena. Components for cube satellites are commercially available to everyone from hobbyists to university researchers and are relatively affordable. Despite the huge ground that has been covered in the electronics to incorporate such capabilities into such a small device, there remains one obstacle that prevents such a technological marvel achieving its full potential: launch costs [1].

Currently the predominant means of launching any payload is through the use of chemical-based propulsion. However the use of chemical propulsion for space exploration is confined to large scale missions as the cost of the propellant to launch a single small payload, such as a cube satellite, into orbit would far surpass the cost of the payload and its systems, hence such the such a mission would be ludicrous to consider as the labour required to launch it into orbit would exceed results of the mission itself, i.e. there would be no profit in conducting such a mission. At present, the cost of launching a < 10 kg payload is in excess of \$ 7 Million [2], and this only takes into account the cost of the propellant itself. As a consequence, small payloads, such as small satellite projects, are often “*piggybacked*” on larger missions, but due to the infrequency of and time frame and planning required to set up large scale missions small projects are often left waiting years till they can launch [2]. It is reported that as of 2015 NASA has launched 30 small satellites whilst they have a backlog of over 50 more waiting to launch as secondary payloads on future missions [3].

Due to the increasing popularity, and more importantly the increasing functionality and capabilities of cube satellites, it is important that we look into the design of an alternative and dedicated launch system for such devices. This report looks into the use of an EMLS (and some aspects that would have to be considered for such a system) as an alternative to launch cube satellites.

3 BACKGROUND

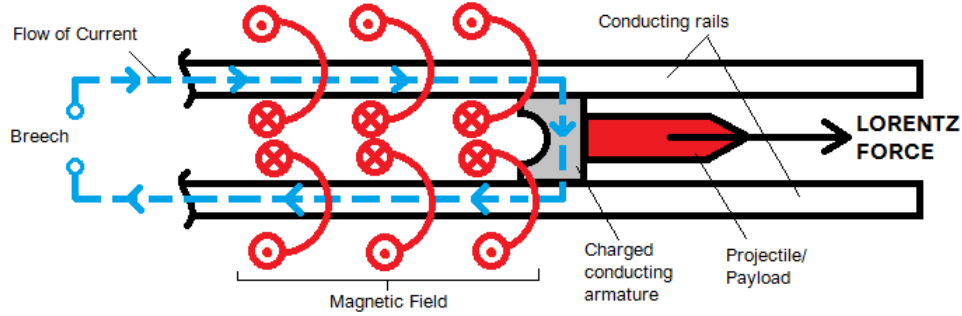
3.1 ELECTROMAGNETIC LAUNCHERS

EMLs have been built and tested successfully since the 1980s and electromagnetic technology has made huge advances. Electromagnetic technology has been used effectively on transport systems such as *Maglev* and bullet trains and on military applications such as Electromagnetic Aircraft Launcher Systems (EMALS) and ballistic applications such as battleship guns [4], [5], [6].

As of the late 1980s railguns have achieved muzzle velocities of up to < 6 km/s for projectiles of mass < 10 kg [7], however the resources required to do so are taxing. EMLs are prevalent in certain ballistic applications in the military, most specifically in Naval warfare. They are used on EMALS and most battleship guns and submarine torpedo launchers because of the fact that the project mass (and hence cost per unit) is significantly lower as they

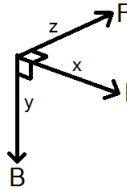
do not require their own propulsive system. However they require significantly lower muzzle velocities compared to launching payloads into space - ballistic applications only require muzzle velocities of approximately 2.5 km/s to 3.5 km/s to effectively breach vehicular armour [8], whilst a launch to space would require in muzzle velocities in excess of 7 km/s to effectively launch a small payload effectively so that it can achieve Low Earth Orbit (LEO) [7], [9], [10].

Figure 1: Diagram showing the formation of Magnetic B-Field and the the consequential Lorentz force that arises due to the field's influence on the charged conducting armature.



Conventional railguns are essentially an extending electrical circuit. This circuit consists of the breech, the two rails and the conducting armature (this is either a solid metal armature or a plasma armature). Current passes from the breech and up one rail and through the armature and down the opposite rail and back to the breech. When a current passes through a wire, or in this case a rail, a magnetic field forms around the charged wire; we can use Maxwell's right hand cork screw rule to ascertain the direction of the field. Since the currents in opposite rails run in opposing directions the magnetic fields generated in either rail oppose each other and hence the rails will oppose each other [1] - this can be seen in figure 1. When an electrically charged body such as a particle, or in this instance the charge armature, is exposed to a B-field it experiences a force known as the Lorentz force, the vector direction of which can be ascertained by *Fleming's Left Hand Rule*. This essentially states that the direction of the Lorentz force will be the cross product of the direction of the current and magnetic field. And since the armature is carrying its own vector charge and the fields on both rails point down in the same direction at the centre of the rails, as a result we have the following setup of components, as shown in figure 2.

Figure 2: Visualisation of cross product of B-field, Current Direction and Lorentz Force vector.



The formula for Lorentz is as follows,

$$F = JB = \frac{1}{2} L' I^2 , \quad (3.1)$$

where L' is the inductance gradient and J is current density defined by

$$J = \frac{I}{A} , \quad (3.2)$$

where A is the cross sectional area perpendicular to the flow of current.

The derivation for magnetic field strength and its effect on Lorentz force is dicussed in greater detail in section 4 CALCULATIONS.

Studies have found that the optimum efficiency of a railgun will never go beyond 50%, as research has shown that the inductive energy that remains in the barrel of the EML is equal to the kinetic energy of the projectile as it leaves the muzzle [11].

$$\frac{1}{2}mv^2 = \frac{1}{2}L'I^2X_{barrel} \quad (3.3)$$

Therefore this would mean that,

$$E_{brech} = E_k + E_i , \quad (3.4)$$

and,

$$\eta = \frac{E_k}{E_{brech}} = 0.5 . \quad (3.5)$$

However this is the maximum *theoretical* efficiency, the real efficiency is closer to $\eta = 0.15$ due to resistive and heating losses [10] - this must be taken into consideration during the design for an EML to launch to space.

3.2 ARMATURES

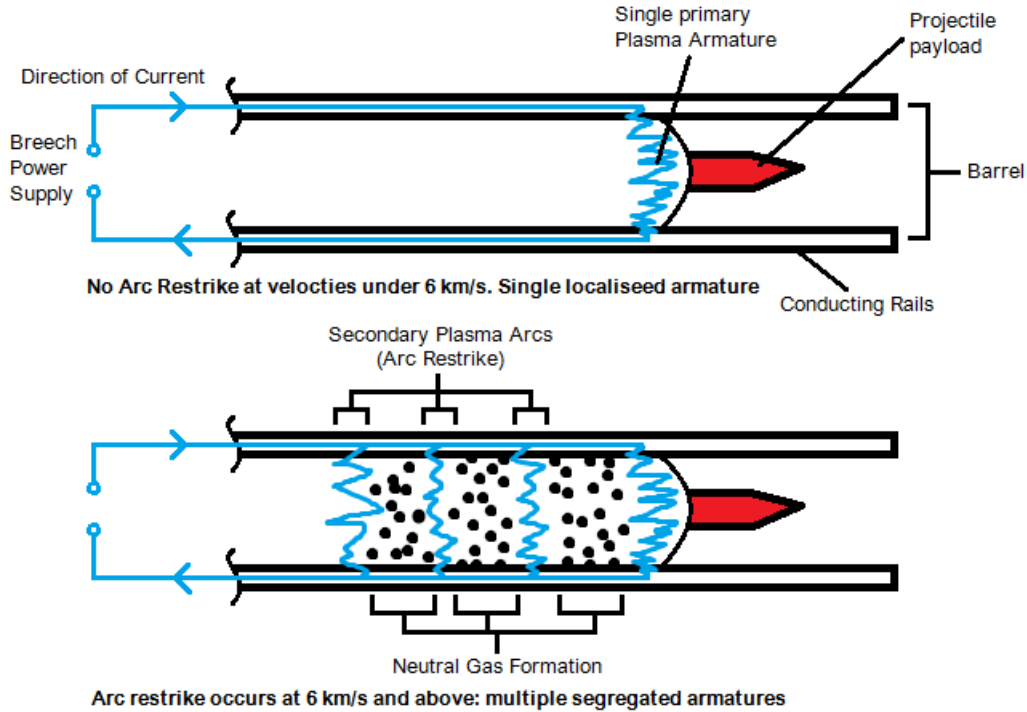
The projectile armature is a part that sits behind the projectile and conducts and carries the current from one rail to the other. As a result of carrying the charge between the two rails, the armature itself becomes charged and hence a Lorentz force is induced and acts on it due to the field that surrounds the charge armature.

During the first designs and testing of EMLs solid metal armatures were used. These could not achieve a velocity beyond 1.5 km/s, as the heat generated by the current and friction would melt the solid metal contacts of the armature causing a Velocity Skin Effect (VSE)[12]. Not only did this slow down the projectile acceleration through the barrel, it also meant that the barrel was degraded very quickly.

Since the 1980s EMLs have been using plasma armatures - these overcome the VSE and achieve muzzle velocities significantly higher than solid armature, easily reaching hypersonic speeds close to 6 km/s. However, therein lies the problem - plasma armatures have simply raised the velocity limitation to 6 km/s; although muzzle velocities of < 6 km/s are more than sufficient for ballistics applications, a launch to space requires at minimum 7 km/s. The advent of the plasma armature has also brought about its own unique problems as well, all of which contribute to the velocity barrier at ~ 6 km/s.

Unless the railgun utilises an evacuated barrel there are the obvious hindrances caused by aerodynamic drag as the projectile is accelerated. The more prominent obstacle is the occurrence of *arc restrike* due to *ablation*.

Figure 3: Diagram showing projectile travelling through barrel at velocities below 6 km/s and above 6 km/s and the resulting arc restrike effects.



Since plasma consists of charged particles including ions and electrons, it can act as a charge carrier. In comparison to solid armatures it is lighter, has reduced friction occurrence and the generated magnetic field will

have a greater influence on it due to the whole armature being charged.

The problem lies in the plasmas fluid like nature combined with the fact that it is ionised. Since it is ionised it is highly reactive with its surroundings, couple this with the fact that the extremely high operating temperatures and pressures within the barrel and an inevitable chemical reaction occurs between the plasma and rail lining. This reaction tends to occur when the velocity of the armature (and projectile) reach ~ 6 km/s. As a result of the reaction with the rail lining a dense neutral gas is formed behind the primary armature. Since there is no means of removing this gas and the magnetic field has no affect on it due to its neutral charge it often traps part of the plasma armature behind it causing a secondary arc to form. This can happen multiple times as seen in figure 3 thus forming multiple secondary arcs - a phenomenon known as arc restrike. In essence, this creates a parallel circuit with multiple points for the current to cross over, thus dividing the total current, I by the n number of secondary armatures. This means that the Lorentz force acting on the primary armature behind the projectile decreases severely when arc restrike occurs [13].

3.3 PROJECTILE DESIGN

The cube satellite cannot simply be launched without a casing or any form of protection or aerodynamic body as it would not be effective in travelling through the atmosphere and will inevitably be damaged in the process. Several design constraints must be taken into account including the size of the satellite itself, the size of the EML bore and the aerodynamic shape of the body that will encase the cube satellite [1]. This report will look at the latter, specifically the design of the projectile casing's nose cone. It will look at the pressure around three different nose cones; these are the following:

- Elliptical
- Haack
- Von Karman

The aerodynamic shape of the projectile nose cone will be essential in reducing drag, especially since the projectile will leave the muzzle of the EML at hypersonic speeds. The launch itself will take place at high altitudes - a launch from ground via EML would be conducted at an altitude of 3 km [1] - hence the density of the air would be lower but would still have a substantial effect on the aerodynamic forces due to the hypersonic exit velocities.

4 CALCULATIONS

4.1 THE BIOT-SAVART LAW

Figure 4: 2-Dimensional coordincate setup of railgun, armature and breech.

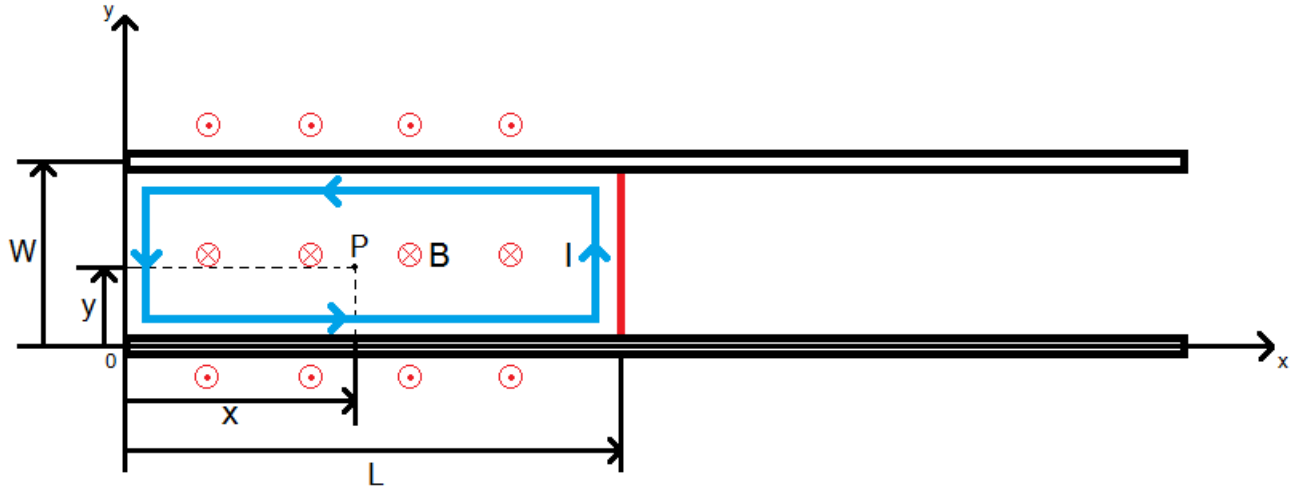
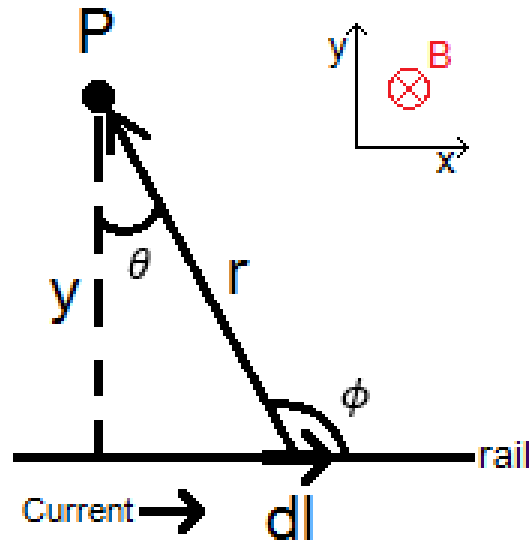


Figure 5: Close-up of some position P between armature and the EML rails.



This section will look at the derivation to calculate magnetic field strength, B at some point P between the rails at some instance where the armature is at a distance L from the breech. The EML setup and the coordinate system applied to it are shown in figures 4 and 5.

The general formula for magnetic field strength at P for a steady current is given as the following using the Biot-Savart law [14],

$$B(P) = \frac{\mu_0 I}{4\pi} \int \frac{d\vec{l} \times \hat{r}}{r^2} , \quad (4.1)$$

where μ is permeability of free space, I is the current through the wire (i.e. rails). The expression $d\vec{l} \times \hat{r}$ is the cross vector for the two vectors \vec{l} and the vector form of r . Taking \hat{r} as one, the expression can be rewritten as the following,

$$d\vec{l} \times \hat{r} = dl \cdot \sin \phi . \quad (4.2)$$

And based on figure 5 we know that $\sin \phi = \cos \theta$, hence we can write equation 4.2 as the following,

$$d\vec{l} \times \hat{r} = dl \cdot \cos \theta . \quad (4.3)$$

From figure 5 we can also see that the following expression is true,

$$\tan \theta = \frac{l}{y} , \quad (4.4)$$

Therefore,

$$\frac{dl}{d\theta} = y \sec^2 \theta , \quad (4.5)$$

which can be rewritten as,

$$dl = \frac{y}{\cos^2 \theta} d\theta . \quad (4.6)$$

Using trigonometry it can also be deduced that

$$\cos \theta = \frac{y}{r} \quad (4.7)$$

And therefore,

$$\frac{1}{r^2} = \frac{\cos^2 \theta}{y^2} \quad (4.8)$$

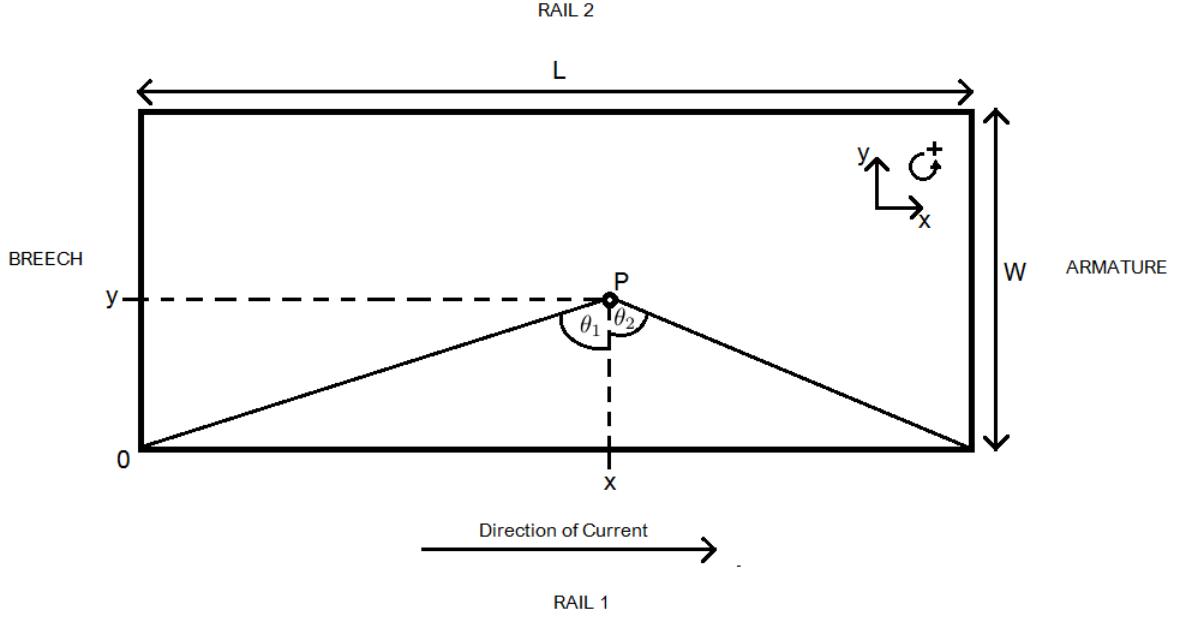
Substituting equations 4.3 and 4.8 into equation 4.1, and integrating between a starting angle θ_1 and end angle θ_2 , we get the following expression,

$$B(P) = \frac{\mu_0 I}{4\pi} \frac{1}{y} \int_{\theta_1}^{\theta_2} \cos \theta \, d\theta . \quad (4.9)$$

Which finally provides us with the following expression for magnetic field strength at a point P :

$$B(P) = \frac{\mu_0 I}{4\pi y} (\sin \theta_2 - \sin \theta_1) \quad (4.10)$$

Figure 6: Diagram showing θ_1 and θ_2 for some position P relative to position x in railgun circuit loop.



A visual representation of equation 4.10 can be seen in figure 6; This representation allows us to cover the full effective length of a rail at a given time when the armature is at a distance of L from the breech. As the value of L increases (which means the armature moves further down the rail) the value of θ moves closer to 90° . Hence we can say that for an infinitely long wire (or rail) on a domain of $-\infty < x < \infty$,

$$\lim_{x \rightarrow -\infty} \theta(x) = -\frac{\pi}{2}$$

and

$$\lim_{x \rightarrow \infty} \theta(x) = \frac{\pi}{2} .$$

Hence if we integrate equation 4.9 with the following limits we achieve the following,

$$B(P) = \frac{\mu_0 I}{4\pi y} \int_{-\frac{\pi}{2}}^{\frac{\pi}{2}} \cos \theta \, d\theta \quad (4.11)$$

$$B = \frac{\mu_0 I}{4\pi y} \sin \theta \bigg|_{\theta=-\frac{\pi}{2}}^{\theta=\frac{\pi}{2}} \quad (4.12)$$

$$B = \frac{\mu_0 I}{4\pi y} \left[\sin \left(\frac{\pi}{2} \right) - \sin \left(-\frac{\pi}{2} \right) \right] .$$

Hence we finally achieve the general expression for the Biot-Savart Law for magnetic field strength.

$$B = \frac{\mu_0 I}{2\pi y} \quad (4.13)$$

4.2 MAGNETIC FIELD STRENGTH IN A RAIL GUN

The general Biot-Savart equation (equation 4.13) only applies to a single infinitely long wire on a one dimensional plane. We can calculate the total magnetic field strength at P splitting the circuit in figure 4 into four individual wires [15] (and therefore currents) and integrating them with real limits using equation 4.9. These are the following:

- Current through the breech
- Current through rail 1
- Current through rail 2
- Current through the armature

The sum of the above fields will give the total field strength of the system for a constant current. However as the charged armature will only be affected by the fields from the rails either side of the armature we need not calculate the magnetic field strength from the breech or the armature as, based on Flemings left hand rule, the influence they will have on the armature is zero to negligible, hence we only need consider that of the rails.

We can calculate the magnetic field strength in the form of equation 4.10, restated below.

$$B(P) = \frac{\mu_0 I}{4\pi y} (\sin \theta_2 - \sin \theta_1)$$

where θ_1 would be the angle between the current origin point on the finite wire and the x -coordinate of the point P and θ_2 would be the angle between current end point and the x -coordinate of the point P and the armature end of the rail as can be seen in 6. The following reasoning will be based on the coordinate setup in figures 4 and 6.

In order to use equation 4.10, values of $\sin \theta_1$ and $\sin \theta_2$ must be discerned. This can simply done through evaluating trigonometric relationships in figures 4, 5, and 6.

Taking the coordinates of point P as (x, y) , the distance between armature and breech as L and the rail separation as W (as seen in figure 6), we can use the Pythagoras theorem to determine relations ships between θ_1 and θ_2 and the lengths opposite to them. When discerning the length we must ensure to take the vector direction of said length *relative to the circuit loop* and not simply magnitude and direction on the 1-dimensional x -plane.

Hence starting with the lower rail (rail 1 in figure 4), we can deduce that

$$\sin \theta_1 = \frac{-x}{\sqrt{x^2 + y^2}} \tag{4.14}$$

and

$$\sin \theta_2 = \frac{L - x}{\sqrt{y^2 + (L - x)^2}} \tag{4.15}$$

therefore

$$B(P)_{rail1} = \frac{\mu_0 I}{4\pi y} \left(\frac{L - x}{\sqrt{(L - x)^2 + y^2}} + \frac{x}{\sqrt{x^2 + y^2}} \right) \tag{4.16}$$

For the upper rail (rail 2), θ_1 and θ_2 would switch sides since the current is flowing from right to left, and the vertical distance from rail 2 to point P is $W - y$ hence we would have the following expressions,

$$\sin \theta_1 = \frac{-x}{\sqrt{x^2 + (W - y)^2}} \quad (4.17)$$

and

$$\sin \theta_2 = \frac{L - x}{\sqrt{(L - x)^2 + (W - y)^2}} \quad (4.18)$$

therefore,

$$B(P)_{rail2} = \frac{\mu_0 I}{4\pi(W - y)} \left(\frac{L - x}{\sqrt{(L - x)^2 + (W - y)^2}} + \frac{x}{\sqrt{x^2 + (W - y)^2}} \right) \quad (4.19)$$

We could also calculate B_{brech} and $B_{armature}$ however due to Fleming's Left Hand rule we know that the field that arises through the armature and brech will have negligible contribution to the Lorentz force that arises on the armature. Hence that total magnetic field strength at a random point P within the electrical loop, for a steady current is given by the following,

$$B(P)_{total} = B_{rail1} + B_{rail2}$$

$$\begin{aligned} B(x, y, L, W, I)_{total} = & \frac{\mu_0 I}{4\pi} \left[\frac{1}{y} \left(\frac{L - x}{\sqrt{(L - x)^2 + y^2}} + \frac{x}{\sqrt{x^2 + y^2}} \right) \right. \\ & \left. + \frac{1}{W - y} \left(\frac{L - x}{\sqrt{(L - x)^2 + (W - y)^2}} + \frac{x}{\sqrt{x^2 + (W - y)^2}} \right) \right] \end{aligned} \quad (4.20)$$

Equation 4.20 provides the general expression for the effective field that will accelerate a charged body parallel to the x -axis seen in figure 4. In order get an equation specific to the magnetic field influence on point on the armature we simply substitute $x = L$, L being the distance of the armature from the brech.

$$B(y, L, W, I)_{total} = \frac{\mu_0 I}{4\pi} \left(\frac{L}{y\sqrt{L^2 + y^2}} + \frac{L}{(W - y)\sqrt{L^2 + (W - y)^2}} \right) \quad (4.21)$$

4.3 THE LORENTZ FORCE

Once the magnetic field strength has been calculated for a point on the armature using the Biot-Savart Law, we can calculate the *Lorentz Force* for a steady current using the following equation,

$$F(L, W, I) = I \int d\vec{y} \times \vec{B}(y, L, W, I) , \quad (4.22)$$

it is the cross product of the B -field vector and the current direction vector. Since the direction of the current is remains constant and the vector direction of y is assumed uniform as well, we can simply take the vectors in the integral of equation 4.22 as magnitudes of their respective variables and simply multiply the total integral by a unit vector of $\hat{x} = 1$ in the x axis direction shown in figure 4 [15]. Therefore substituting equation 4.21 into equation 4.22 would yield the magnitude (and vector) solution that arises on armature as a result of the magnetic field induced by the effective length, L of the rail (Note: we must remember that L is simply the displacement of the armature from the breech at a specific time, and hence is a time dependent variable, but it is being taken at as a constant at a time t).

$$F(I, L, W)_{total} = \frac{\mu_0 I^2}{4\pi} \hat{x} \int \left(\frac{L}{y\sqrt{L^2 + y^2}} + \frac{L}{(W-y)\sqrt{L^2 + (W-y)^2}} \right) dy \quad (4.23)$$

Through various integration methods we get the following solution for the Lorentz force integral (the full derivation for equation 4.24 can be found in APPENDIX I):

$$F(I, L, W)_{total} = \frac{\mu_0 I^2}{4\pi} \hat{x} \left(\frac{1}{2} \ln \left| 1 - \frac{2L}{\sqrt{L^2 + y^2} + L} \right| + \ln \left| \frac{L}{W-y} + \sqrt{\frac{L^2}{(W-y)^2} + 1} \right| \right) . \quad (4.24)$$

We cannot simply substitute in the limits for the integral solution in equation 4.24 as being $y = 0$ to $y = W$ since this would not give a real result. Such an action would give us $\ln(0)$ terms; this is not a defined value. This is simply explained by the fact that the y displacements $y = 0$ and $y = W$ are mathematically the exact precise y -coordinates for the exact centres of rail 1 and rail 2 respectively, where it is assumed the B -field has infinite strength. In a real life situation we will never be able to approach the B -field exactly at $y = 0$ and $y = W$, since it is a physical impossibility. Hence when integrating, the limits for y must satisfy the the following mathematical inequality,

$$0 < y < W , \quad (4.25)$$

especially noting that y always satisfies the statements $y \neq 0$ and $y \neq W$.

From the equation 4.24 we can also calculate the acceleration of the projectile (assuming there are no drag or friction forces acting on the body) by simply using the $F = Ma$, since $F(I, L, W)_{total} = Ma$ where M would be the total combined mass of the projectile body and armature and a would be the acceleration of those bodies. Furthermore, relating $F(I, L, W)_{total}$ to equation 3.1 we can also find the inductance gradient for a steady current I and using equation 4.21 with equation 4.25 we can also calculate current density, J for a steady current, which would in turn allow us to calculate the size of the contact are between the armature and rails, using equation 3.2.

4.4 STEADY CURRENT

Up until this point we have assumed that the EML will use a constant current to function. The definition of a constant current is that the current through the rails will immediately start at a current of $I = I_0$ at a time $t = 0$ and will drive the armature (and projectile) with a consistent current of I up until a time $t = T$, at which it is exact point that the projectile armature leaves the barrel of the EML and the current will immediately go back to $I = 0$ [16]. This is an ideal case for a device such as an EML since it would ensure that the armature is under the influence of a constant and unchanging Lorentz force, maximising the muzzle exit velocity of the projectile. However such a power supply would use huge amounts of energy and (based on the research conducted by McNab [10] who says that current plasma based EMLs have an approximate efficiency of $\eta = 0.15$) would be very inefficient, since most of the energy would either be dissipated as heat or would remain in the barrel as inductive energy.

Equation 3.1 and Newton's Second Law (i.e. $F = Ma$) can be used together to calculate the the acceleration of the armature and projectile, or alternatively find the steady current required for a desired acceleration. Further propagation of equation 3.1 would provide us with the means to calculate the total charge Q delivered to system running at a steady current I in a time T [16].

The standard equation for charge is given as follows,

$$Q = It . \quad (4.26)$$

Hence equation 3.1 can be rewritten as,

$$F = Ma = \frac{1}{2} L' \left(\frac{Q}{t} \right)^2$$

therefore,

$$a = \frac{1}{2} \frac{L'}{M} \left(\frac{Q}{t} \right)^2 . \quad (4.27)$$

Given that the Lorentz force takes affect after an initial velocity, v_0 we can derive the expression for the velocity at a time t as being,

$$\begin{aligned} v &= v_0 + \frac{1}{2} \frac{L'}{M} \frac{Q^2}{t} \\ &= v_0 + \frac{1}{2} \frac{L'}{M} IQ , \end{aligned} \quad (4.28)$$

and from this we can derive an expression for the displacement given that the projectile has an initial displacement of x_0 (it is important to note that v_0 and x_0 will not necessarily always be zero - this will be discussed later - but for the purposes of these derivations assume that v_0 and x_0 are equal to zero).

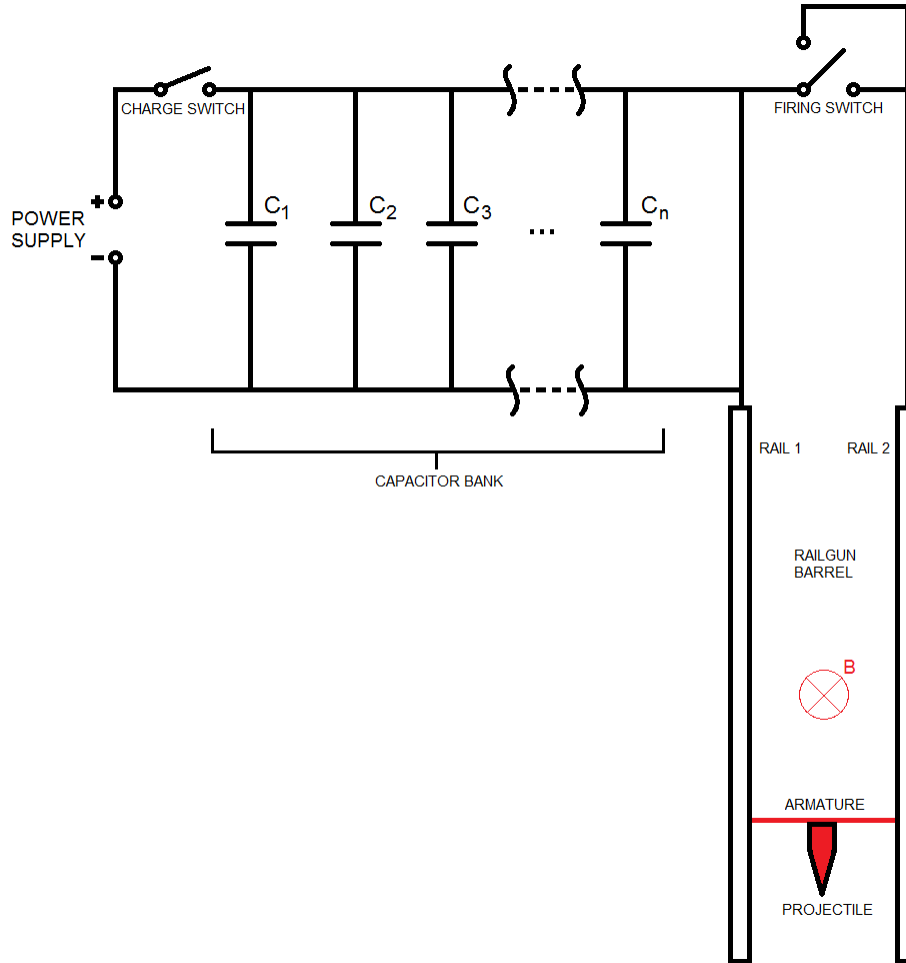
$$x = x_0 + v_0 t + \frac{1}{4} \frac{L'}{M} Q^2 \quad (4.29)$$

In reality, a current will always take some time to charge up to it peak and it is no different for an EML circuit. If anything its effects are more pronounced due to magnitude of current an EML requires in order to function.

4.5 PULSED CURRENT

The steady current scenario assumes that the EML circuit is a simple circuit with few components other than a power DC power supply and the electromagnet itself (which is essentially an inductor). Although a circuit such as this is theoretically feasible, it would require unfathomable amounts of energy to function and further sustain. A more realistic circuit for an EML is that of an LC circuit (i.e. an Inductor Capacitor circuit). This incorporates a capacitor into the basic EML circuit. The capacitor component(s) would be incorporated into the breech end of the EML seen in figure 1 and would be the link between two circuits as show in figure 7. This capacitor component would be some form of capacitor bank with n number of capacitors which, while disconnected from the railgun segment of the circuit, can be charged up using a power generator. Once charged the capacitor bank is disconnected from the power supply and connected to the EML segment of the circuit, through which the charged capacitor bank discharges to power the railgun.

Figure 7: A simple LC railgun circuit consisting of capacitor bank connected to power generator which is used to charge the capacitor bank via the charge switch connection. Once fully charged the charge switch opens and the firing switch disconnects from the charging circuit to the discharging circuit, allowing the charge stored in the capacitor bank to discharge and power the EML circuit.



The circuit shown in figure 7 will discharge too quickly for the current to have a prominent effect on generating the Lorentz force; in order to prolong this a resistor component should be incorporated into the circuit to form an RLC circuit.

Charging the capacitor bank up to the peak current is given by the expression

$$I = I_0 \sin(\omega t) \quad (4.30)$$

where

$$\omega = \frac{1}{\sqrt{LC}} , \quad (4.31)$$

ω being the natural frequency, and I_0 is the peak current [16], [17].

The discharge current once the firing switch is closed is given by the following,

$$I = I_0 e^{-\frac{R}{L}t} . \quad (4.32)$$

Based on equation 4.30 we know that the peak current during charging of the capacitor bank occurs when $\sin(\omega t) = 1$ which must mean that $\omega t = \frac{\pi}{2}$, and using equation 4.31 we can say that

$$\frac{t'}{\sqrt{LC}} = \frac{\pi}{2}$$

t' being the time it takes to charge the capacitor bank to I_0 . From this we can rearrange to find t' .

$$t' = \frac{\pi}{2} \sqrt{LC} . \quad (4.33)$$

Substituting equation 4.30 into equations 4.27, 4.28, 4.29 gives us the equations for acceleration, velocity, and displacement at time t due to the pulsed power source's capacitor bank charging stage.

Acceleration at time t' is

$$a(t') = \frac{1}{2} \frac{L'}{M} I_0^2 \sin^2(\omega t') . \quad (4.34)$$

Hence velocity at time t' is given by

$$\begin{aligned} v(t') &= v_0 + \int_0^{t'} a(t) dt \\ &= v_0 + \frac{1}{2} \frac{L'}{M} I_0^2 \int_0^{t'} \sin^2(\omega t) dt \\ &= v_0 + \frac{1}{2} \frac{L'}{M} I_0^2 \int_0^{t'} \left(\frac{1}{2} - \frac{1}{2} \cos(2\omega t) \right) dt \\ &= v_0 + \frac{1}{2} \frac{L'}{M} I_0^2 \left[\frac{1}{2} t - \frac{1}{4\omega} \sin(2\omega t) \right]_0^{t'} \\ v(t') &= v_0 + \frac{1}{2} \frac{L'}{M} I_0^2 \left[\frac{1}{2} t' - \frac{1}{4\omega} \sin(2\omega t') \right] . \end{aligned} \quad (4.35)$$

And therefore displacement at time t' is given by

$$\begin{aligned}
x(t') &= x_0 + \int_0^{t'} v(t) dt \\
&= x_0 + \int_0^{t'} \left(v_0 + \frac{1}{4} \frac{L'}{M} I_0^2 t - \frac{1}{8\omega} \frac{L'}{M} I_0^2 \sin(2\omega t) \right) dt \\
&= x_0 + \left[v_0 t + \frac{1}{8} \frac{L'}{M} I_0^2 t^2 + \frac{1}{16\omega^2} \frac{L'}{M} I_0^2 \cos(2\omega t) \right]_0^{t'} \\
x(t') &= x_0 + v_0 t' + \frac{1}{8} \frac{L'}{M} I_0^2 t'^2 + \frac{1}{16\omega^2} \frac{L'}{M} I_0^2 \cos(2\omega t') .
\end{aligned} \tag{4.36}$$

Since $\omega t' = \frac{\pi}{2}$, we can substitute these into equations 4.34, 4.35, and 4.36. Therefore we have the following equations

$$a(t') = \frac{I_0^2 L'}{2M} , \tag{4.37}$$

$$v(t') = v_0 + \frac{\pi I_0^2 L' \sqrt{LC}}{8M} , \tag{4.38}$$

$$x(t') = x_0 + \frac{\pi}{2} v_0 \sqrt{LC} - \frac{\pi^2 I_0^2 L' LC}{32M} . \tag{4.39}$$

Once the current discharges from the capacitor bank, the inductive energy of the EML circuit does not reach zero, i.e. the inductive energy in the barrel reaches zero at $t = \infty$. The following equation can be used to calculate a fraction of the peak current I_0 that is a desirable current to be left over in the EML once the projectile has launched.

$$f I_0 = I_0 e^{\frac{R}{L} \Delta t} , \tag{4.40}$$

where f is the fraction coefficient. Rearranging equation 4.40 will give us the time taken for the current to drop from peak charge to f fraction of the peak charge.

$$\Delta t = -\frac{L}{R} \ln(f) , \tag{4.41}$$

where $\Delta t = t_f - t'$. According to Feliciano a desirable fraction coefficient for a railgun circuit is approximately $f = 0.175$.

Similar to equation 4.30 we can substitute equation 4.32 into equations 4.27, 4.28, and 4.29 to find acceleration, velocity and displacement respectively, during the discharging phase [16] for a time t and for fraction coefficient time t_f .

Acceleration is given by

$$a(t) = \frac{1}{2} \frac{L'}{M} I_0^2 e^{-2t \frac{R}{L}} , \tag{4.42}$$

and

$$a_f = \frac{1}{2} \frac{L'}{M} f^2 I_0^2 . \quad (4.43)$$

Velocity is given by

$$v(t) = v_0 + \frac{1}{2} \frac{L'}{M} I_0^2 \int e^{-2(t-t') \frac{R}{L}} dt \quad (4.44)$$

$$v_f = v_0 - \frac{1}{4} \frac{L'}{M} \frac{L}{R} I_0^2 e^{-2(t-t') \frac{R}{L}} \Bigg|_{t'}^{t_f} . \quad (4.45)$$

Displacement is given by,

$$x(t) = x_0 + \int \left(v_0 - \frac{1}{4} \frac{L'}{M} \frac{L}{R} I_0^2 e^{-2(t-t') \frac{R}{L}} \right) dt \quad (4.46)$$

$$x_f = x_0 + v_0 t + \frac{1}{8} \frac{L'}{M} \frac{L^2}{R^2} I_0^2 e^{-2(t-t') \frac{R}{L}} \Bigg|_{t'}^{t_f} . \quad (4.47)$$

5 SIMULATIONS

5.1 ASSUMPTIONS AND PARAMETERS

Some simulations were run on MATLAB for steady current and the pulsed current. In regards to the launch parameters, we will make use of very arbitrary values, only for the purposes of demonstration. The simulations were run with the following parameters and assumptions:

- The rail separation W is 25 cm.
- The barrel width is 15 cm.
- The desired acceleration is 250 km/s.
- There is no occurrence of arc restrike.
- There are no frictional or drag forces acting against the projectile
- The EML uses an evacuated barrel.
- The weight of the projectile and armature were ignored in regards to the resultant force that arises, since in comparison to the Lorentz force the weight of the projectile body is minuscule, hence the resultant force is simply the total Lorentz force.
- There are no external forces acting on the projectile body, other than the thrust force from the armature.
- The armature (and projectile) were accelerated from rest ($x_0 = 0$, $v_0 = 0$) only by the Lorentz force.
- The desired orbital altitude of the cube satellite is 450 km.
- This is a single stage launch straight into orbit.
- The projectile has a mass of 10 kg.
- The Earth is not rotating about its axis.
- The launch takes place at sea level.

Assuming that the orbit altitude will be 450 km and that there are no external forces acting on the projectile (i.e. no drag, friction etc.), we can use some basic equations to deduce the launch velocity and angle.

To launch to a vertical height of 450 km from rest ($g = 10 \text{ N/kg}$),

$$\begin{aligned}v_r &= \sqrt{2gs} \\&= \sqrt{2 \cdot g \cdot 450 \cdot 10^3} \\v_r &= 3000 \text{ m/s} .\end{aligned}$$

To stay in orbit the tangential velocity of the launch must be as follows,

$$\begin{aligned}\frac{mv_\theta^2}{r} &= \frac{GMm}{r^2} \\ v_\theta &= \sqrt{\frac{GM}{r}} \\ v_\theta &= \sqrt{\frac{6.674 \cdot 10^{-11} \cdot 5.972 \cdot 10^{24}}{6400 \cdot 10^3}} \\ v_\theta &\approx 8000 \text{ m/s} .\end{aligned}$$

And therefore the launch velocity would be approximately $v_L \approx 8.5 \text{ kn/s}$ at an angle of $\theta_L \approx 21^\circ$.

The energy required for such a feat based on the assumptions would be

$$\begin{aligned}E_{tot} &= \frac{1}{2}mv_L^2 \\ E_{tot} &= 360 \text{ MJ} .\end{aligned}$$

Assuming the EML uses a 20 kV power supply [10], the total capacitance required for the capacitor bank is given by

$$\begin{aligned}E_{tot} &= \frac{1}{2}C_{tot}V^2 \\ C_{tot} &= \frac{2E_{tot}}{V^2} \\ &= \frac{2 \cdot 360 \cdot 10^6}{20000^2} \\ C_{tot} &= 1.80 \text{ F} .\end{aligned}$$

The typical inductance for a two rail geometry is approximately $L = 0.50 \text{ } \mu\text{H}$ [18] and a resistance of $R = 0.00003 \text{ } \Omega$ will be used in order to better see the current pulse profile.

5.2 MATLAB SIMULATIONS

Figure 8: Graph showing Magnetic Field Strength B across the back of armature for a steady current as the armature leaves the EML barrel at a velocity of 8500 m/s.

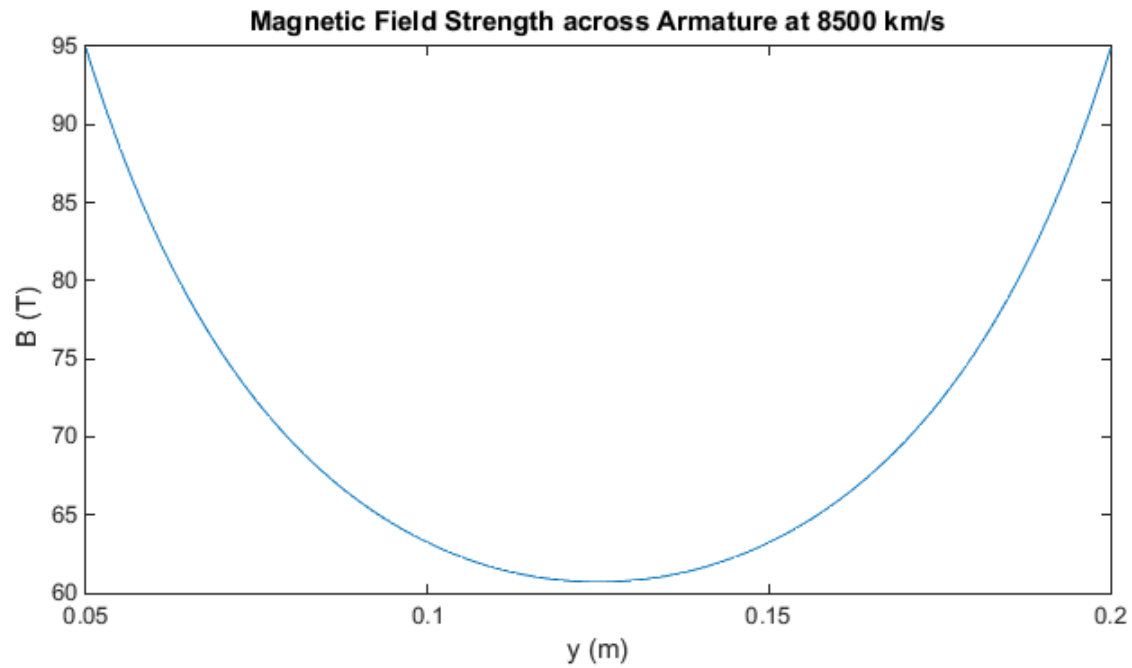


Figure 9: Graph showing Lorentz Force Magnitude across the back of armature for a steady current as the armature leaves the EML barrel at a velocity of 8500 m/s.

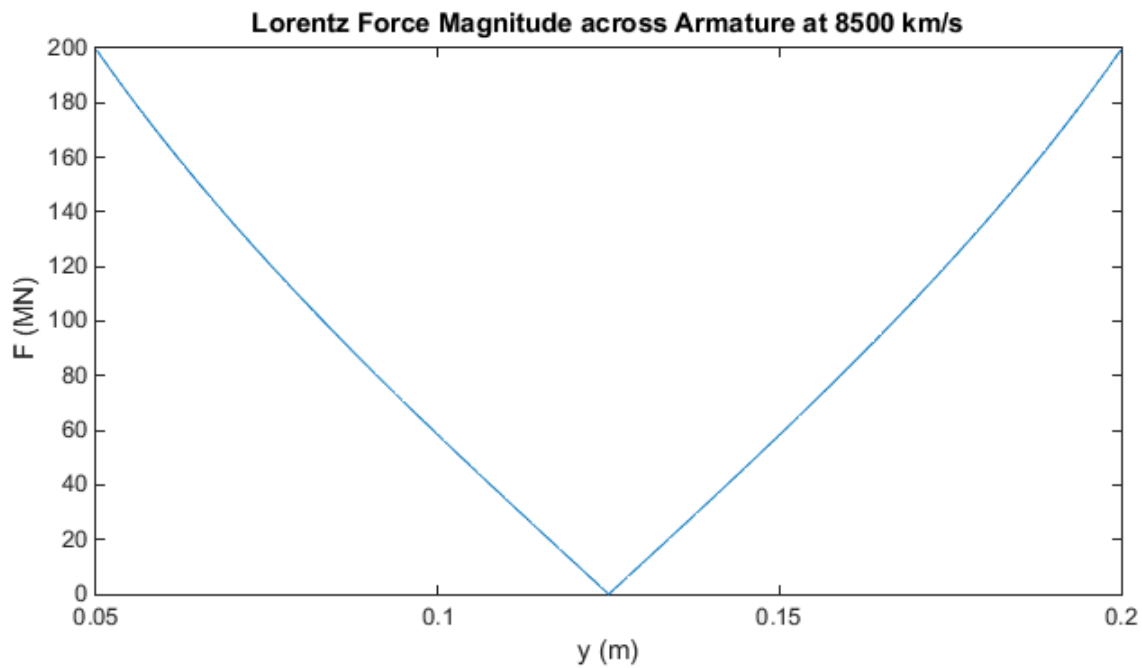


Figure 10: Graph showing charging and discharging phase of pulsed current. Pulse reaches a peak after which the RLC circuit switches to discharge phase where the charge stored on the capacitor banks is discharged through the induction stage, i.e. the EML barrel.

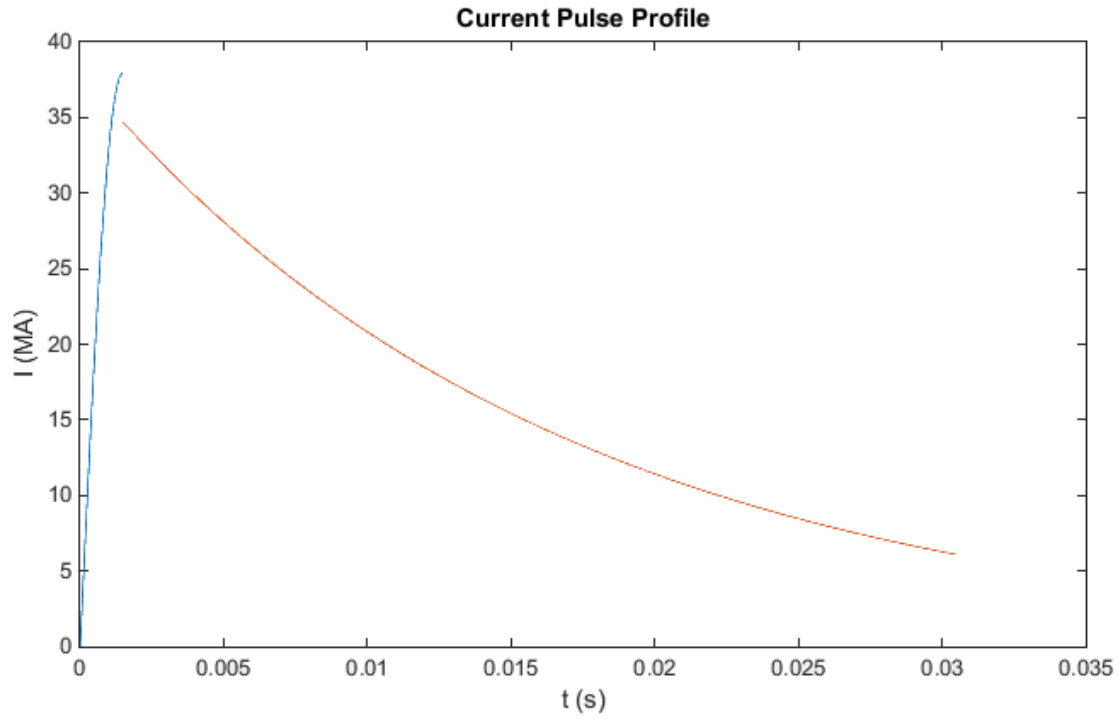
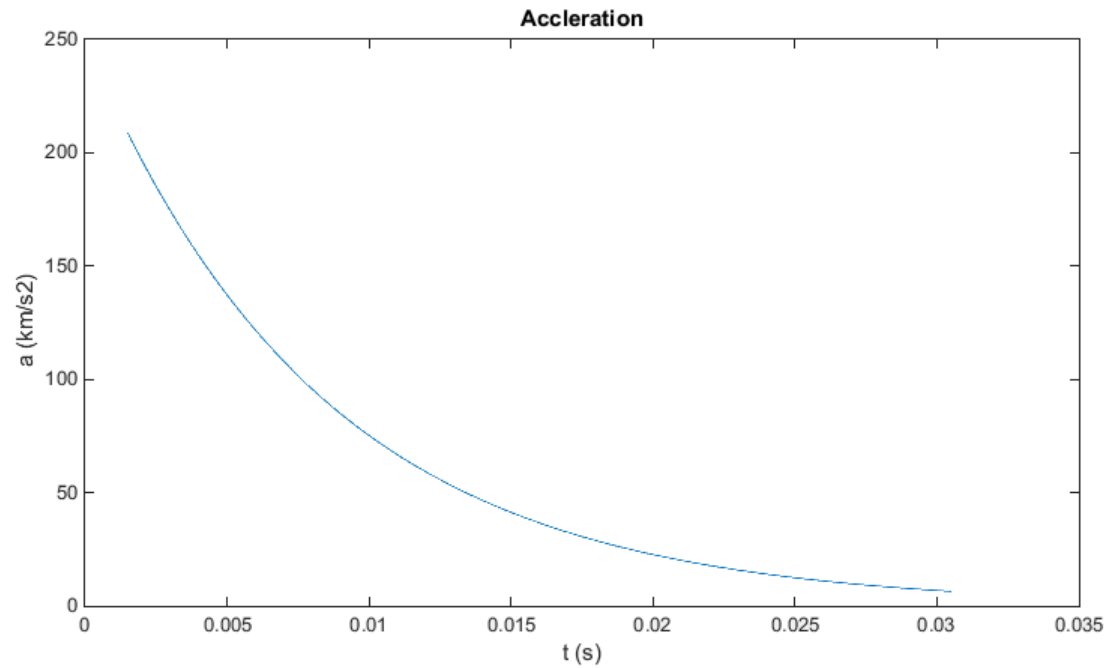


Figure 11: Graph showing acceleration of armature during the discharge phase.



6 DISCUSSION

EMLs as a means to launch small projectiles into orbit show promise as being an alternative means of launch, but the energies required to do so will be expensive and the viability of EMLs as an alternate means of launch, regardless whether it is for small payloads or large ones will depend on the expenses that are required for such a feat.

The assumptions and parameters used to model the figures 8, 9, 10 and 11 are all very ideal (and also highly unlikely) scenarios, however the graphs produced depict some idea of the absolute minimum requirements of such a launch.

Although figure 8 and figure 9 show the magnetic field profile and Lorentz force profile, respectively for the back of the armature when it is at muzzle exit velocity, they both depict the expected profile for magnetic field strength and Lorentz force for any velocity (regardless whether it is under the influence of a steady current or pulsed current) at which the armature (and projectile) are under the influence of the magnetic field in the railgun. When comparing figures 8 and 9 it would appear that the Lorentz force is the derivative of the magnetic field strength, however based on equations 4.22 and 4.23, this is not the case. Looking carefully at figure 9 we can see that the lines curve slightly which is likely due to the logarithmic components of equation 4.23, yet they both come to an abrupt end at the centre of the railgun. It is possible that this is due to the conflicting fields, since the current generated in the two rails, although a part of the same inductive circuit, they essentially oppose each other in regards to their relative vector flow directions, hence it may be that they are having a mutual cancelling effect on each other. It must also be noted that the graphs do not start from the centre line of either rail but rather from the boundary edge of the rail, since this would be the area that the armature is affected. Furthermore as explained in the magnetic field derivation, the field essentially reaches a value of infinity at the exact centre of either rail (hence the same would apply to the force) so the scale at the field strength at $0 < y < 0.05$ m and $0.20 < y < 0.25$ m would dwarf the values shown in figure 8. Using this information we can deduce that it would be more favourable to use thinner rails in such a device, or direct the current in such a way that it passes closer to the boundary of the rails.

We can see that the magnetic field strength at ends of the armature are relatively high, peaking at 95 Tesla at either end and reach a value of 60 Tesla at its lowest point, which in turn translates to a peak Lorentz Force magnitude of 200 MN.

Although the magnetic fields seem to be affecting each other due to their opposition, it may appear to be desirable to therefore increase the separation between the rails, this would decrease the inductance gradient and hence reduce the Lorentz force that arises as a result. Hence a desirable compromise is required for the EML to be effective.

Although figures 8 and 9 are based on a steady current simulation, the same profile is expected for a pulsed current, albeit the magnetic field strength, and consequentially the Lorentz force, is likely to be significantly lower at the muzzle exit velocity for a pulsed current in comparison to a steady one. This is further substantiated by the figures 10 and 11. In figure 10 as the discharge stage tapers so does the total acceleration in 11 since magnetic field Lorentz force and hence acceleration is quadratically proportional to current, as presented by equation 4.24.

7 APPENDIX

7.1 APPENDIX I: LORENTZ FORCE INTEGRAL DERIVATION

The following is the full derivation of the integral for the total Lorentz Force see in equation 4.23, to get to equation 4.24.

$$\begin{aligned} F(I, L, W)_{total} &= \frac{\mu_0 I^2}{4\pi} \hat{x} \int_0^W \left(\frac{L}{y\sqrt{L^2 + y^2}} + \frac{L}{(W-y)\sqrt{L^2 + (W-y)^2}} \right) dy \\ &= \frac{\mu_0 I^2}{4\pi} L \hat{x} \left(\int_0^W \frac{1}{y\sqrt{L^2 + y^2}} dy + \int_0^W \frac{1}{(W-y)\sqrt{L^2 + (W-y)^2}} dy \right) \end{aligned}$$

We can take the above equation and approach the two integrals separately. We will first approach solve the following integral.

$$\int \frac{1}{y\sqrt{L^2 + y^2}} dy$$

We will use substitution to solve this integral. Take the following $u = \sqrt{L^2 + y^2}$. Therefore

$$\frac{du}{dy} = \frac{y}{\sqrt{L^2 + y^2}}$$

so

$$du = \frac{y}{\sqrt{L^2 + y^2}} dy$$

and

$$y^2 = u^2 - L^2.$$

And so we have the following integral,

$$\int \frac{1}{u^2 - L^2} du.$$

Separating this into partial fractions we have the following,

$$\begin{aligned} &\int \frac{1}{2L(u-L)} du - \int \frac{1}{2L(u+L)} du \\ &= \frac{1}{2L} \left(\int \frac{1}{u-L} du - \int \frac{1}{u+L} du \right) \end{aligned}$$

Solving the above we get the following,

$$\frac{1}{2L} \left[\ln(u-L) - \ln(u+L) \right]$$

Finally substituting in $u = \sqrt{L^2 + y^2}$ we get the following,

$$\begin{aligned} \int \frac{1}{y\sqrt{L^2 + y^2}} dy &= \frac{1}{2L} \left| \ln(\sqrt{L^2 + y^2} - L) - \ln(\sqrt{L^2 + y^2} + L) \right| \\ &= \frac{1}{2L} \ln \left| \frac{\sqrt{L^2 + y^2} - L}{\sqrt{L^2 + y^2} + L} \right| \\ &= \frac{1}{2L} \ln \left| 1 - \frac{2L}{\sqrt{L^2 + y^2} + L} \right| \end{aligned}$$

Now we move on to the next integral,

$$\int \frac{1}{(W - y)\sqrt{L^2 + (W - y)^2}} dy$$

Similarly to the previous integral, we can use substitution to solve this integral, this time taking $u = \frac{1}{W - y}$. We can better see how u will be substituted in by first rearranging the integral into the following,

$$\int \frac{1}{(W - y)^2 \sqrt{\frac{L^2}{(W - y)^2} + 1}} dy$$

The differential of u is,

$$\frac{du}{dy} = \frac{1}{(W - y)^2}$$

therefore,

$$du = \frac{1}{(W - y)^2} dy .$$

Now that we have the values of u and du we can assemble the following integral using substitution,

$$\int \frac{1}{\sqrt{u^2 L^2 + 1}} du .$$

If we perform the following substitution using $v = uL$ (hence $dv = L du$) we have,

$$\frac{1}{L} \int \frac{1}{\sqrt{v^2 + 1}} dv .$$

Taking $v = \tan(w)$, we have $w = \arctan(v)$ and $dv = \sec^2(w) dw$, so we have,

$$\frac{1}{L} \int \frac{\sec^2(w)}{\sqrt{\tan^2(w) + 1}} dw$$

The trigonometric identity $\tan^2(w) + 1 = \sec^2(w)$ allows us to write the above integral as

$$\frac{1}{L} \int \sec(w) dw .$$

Multiplying the last integral by $\frac{\tan(w) + \sec(w)}{\tan(w) + \sec(w)}$ we have,

$$\frac{1}{L} \int \frac{\sec(w) \tan(w) + \sec^2(w)}{\tan(w) + \sec(w)} dw .$$

Further substituting $\gamma = \tan(w) + \sec(w)$ means that $d\gamma = [\sec(w)\tan(w) + \sec^2(w)] dw$, hence,

$$\frac{1}{L} \int \frac{1}{\gamma} d\gamma$$

this finally yields

$$\frac{1}{L} \ln \gamma .$$

Substituting in $\gamma = \tan(w) + \sec(w)$, we have

$$\frac{1}{L} \ln |\tan(w) + \sec(w)| ,$$

and since $w = \arctan(v)$, substituting this into the last equation gives us the following,

$$\frac{1}{L} \ln |v + \sqrt{v^2 + 1}| .$$

And $v = uL$, therefore,

$$\frac{1}{L} \ln |uL + \sqrt{u^2 L^2 + 1}| ,$$

and finally substituting $u = \frac{1}{W-y}$ back in gives us,

$$\int \frac{1}{(W-y)\sqrt{L^2 + (W-y)^2}} dy = \frac{1}{L} \ln \left| \frac{L}{W-y} + \sqrt{\frac{L^2}{(W-y)^2} + 1} \right| .$$

As we now have both parts of the Lorentz force integral we can finally solve the total integral.

$$\begin{aligned} F(I, L, W)_{total} &= \frac{\mu_0 I^2}{4\pi} L \hat{x} \int \left(\frac{1}{y\sqrt{L^2 + y^2}} + \frac{1}{(W-y)\sqrt{L^2 + (W-y)^2}} \right) dy \\ &= \frac{\mu_0 I^2}{4\pi} L \hat{x} \left(\frac{1}{2L} \ln \left| 1 - \frac{2L}{\sqrt{L^2 + y^2} + L} \right| + \frac{1}{L} \ln \left| \frac{L}{W-y} + \sqrt{\frac{L^2}{(W-y)^2} + 1} \right| \right) + C \\ F(I, L, W)_{total} &= \frac{\mu_0 I^2}{4\pi} \hat{x} \left(\frac{1}{2} \ln \left| 1 - \frac{2L}{\sqrt{L^2 + y^2} + L} \right| + \ln \left| \frac{L}{W-y} + \sqrt{\frac{L^2}{(W-y)^2} + 1} \right| \right) + C \end{aligned}$$

7.2 APPENDIX II: MATLAB CODE FOR SIMULATIONS

Figure 12: MATLAB code for parameters and equations, adapted from [16].

```

clear all

mtot = 10
pi = 3.14159265359;
mu0 = 4*pi*10.^(-7); %magnetic permeability of a vacuum
W = 0.25; %m bore width
y = 0.05:0.001:0.2; %m
a0 = 250000; %m/s2 desired acceleration
v_L = 8500; %m/s muzzle exit velocity
C_tot = 1.80; %Total capacitance of capacitor bank
L_induc = 0.0000005; %inductance of rail geometry
volt0 = 20000 %power supply voltage
L_tot = v_L^2/(2*a0); %total length of rails
R = 0.00003 %Resistance
f = 0.175 %current fraction coefficient
t_prime = pi*sqrt(L_induc*C_tot)/2
delta_t = -(L_induc/R)*log(f)
t_charge = 0:0.00001:t_prime %t' - time to charge capacitor bank
t_discharge = t_prime:0.00001:(t_prime + delta_t)

y1 = 0.05
y2 = 0.20

I0 = volt0.*sqrt(C_tot/L_induc); %steady current

L_primeinduc = (2*mtot*a0)/(I0.^2); %inductance gradient

w = 1 / sqrt(L_induc*C_tot)

%Magnetic field strength across armature (Tesla)
B = ((mu0*I0)/(4*pi)).*(L_tot./(y.*sqrt(L_tot.^2 + y.^2)) + L_tot./((W - y).*sqrt(L_tot.^2 + (W - y).^2)));

%Lorentz Force across armature (Newtons)
F_Lz = abs(((mu0*(I0.^2))/(4*pi)).*(0.5.*log(1 - ((2*L_tot)/(L_tot + sqrt(L_tot.^2 + y.^2)))) + log((L_tot)/(W - y)) + sqrt(1 + ((L_tot.^2)/(W - y).^2)))));

a2 = 0.5*(L_primeinduc/mtot)*(I0.^2)*exp(-2*t_discharge*R/L_induc)

%Pulse Current Profile
I_charge = I0.*sin(w*t_charge);
I_discharge = I0.*exp(-(R/L_induc).*t_discharge)

%B-field strength at point just before muzzle exit
figure(1)
gcf = plot(y,B)
title('Magnetic Field Strength across Armature at 8500 km/s')
xlabel('y (m)'),ylabel('B (T)')
axis([0.05,0.2,60,95])
hold on

```

Figure 13: MATLAB code to plot graphs for equations.

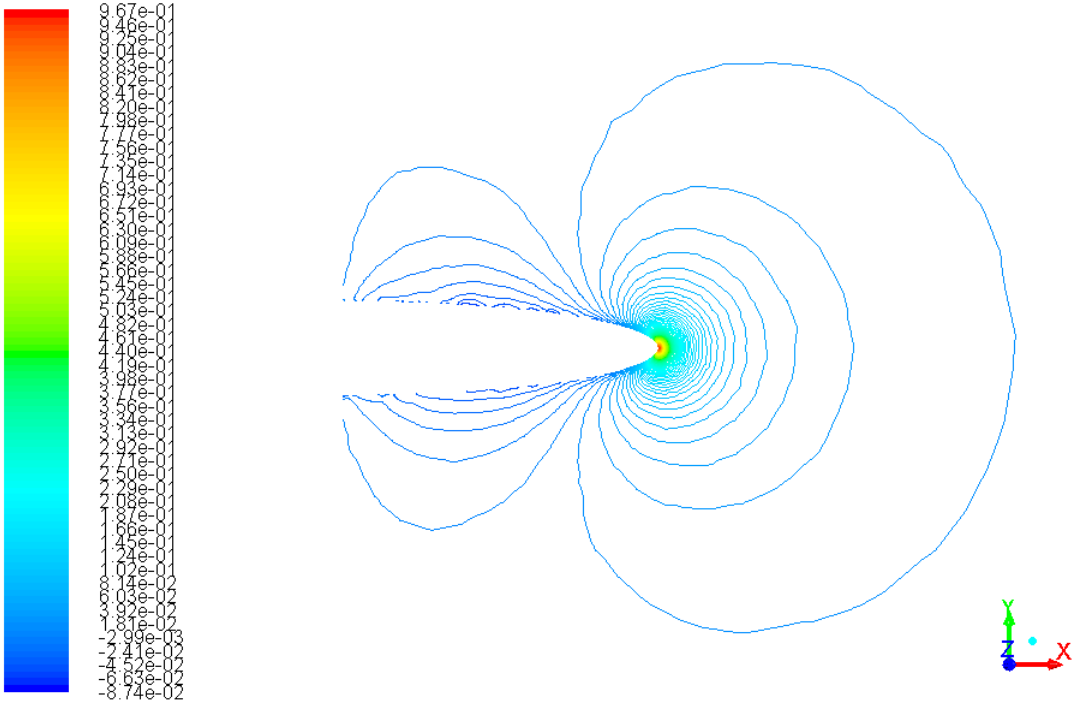
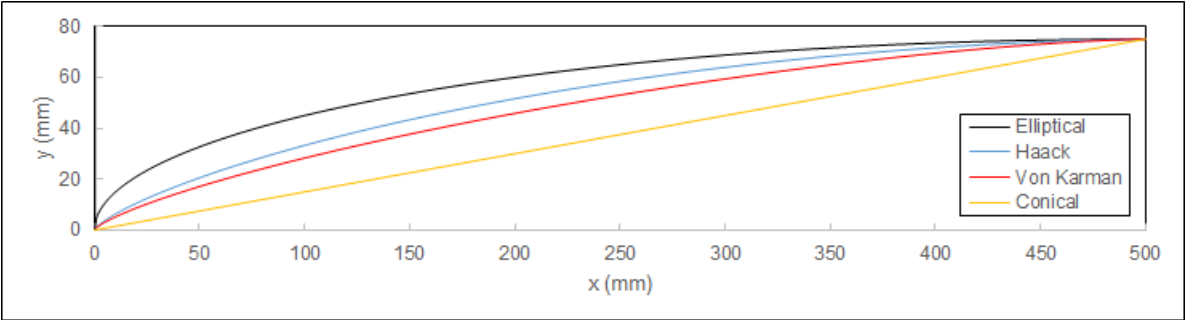
```
%Lorentz force magnitude across armature just before muzzle exit
figure(2)
gcf = plot(y, (F_Lz/1000000))

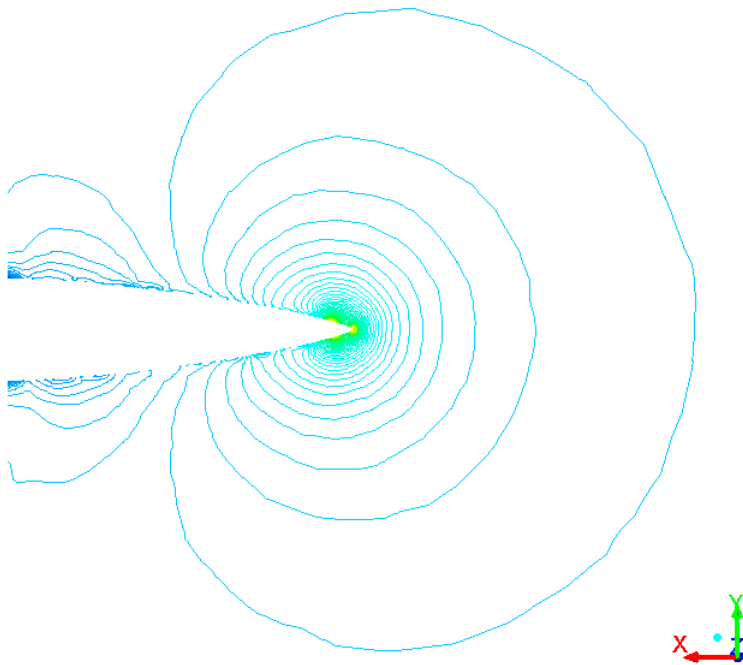
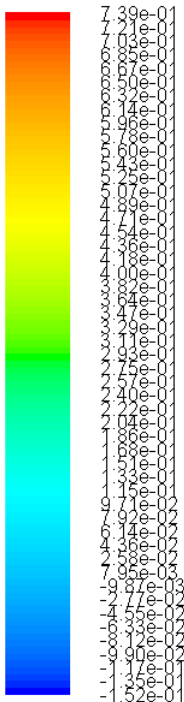
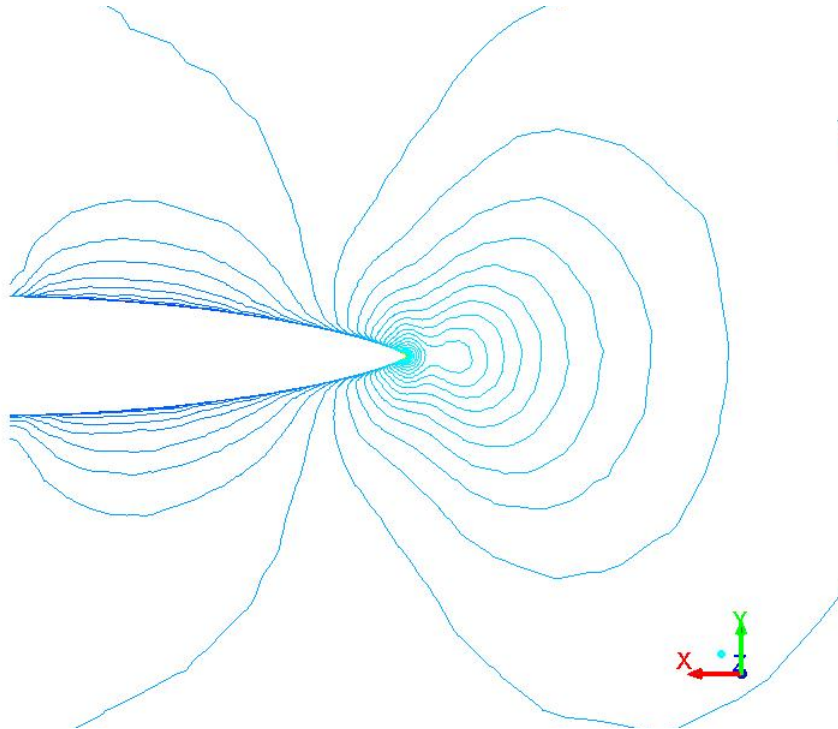
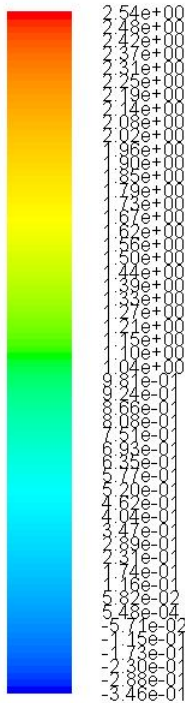
title('Lorentz Force Magnitude across Armature at 8500 km/s')
xlabel('y (m)'), ylabel('F (MN)')
axis([0.05, 0.2, 0, 200])
hold on

%current pulse
figure(3)
gcf = plot(t_charge, (I_charge/1000000), t_discharge, (I_discharge/1000000))
title('Current Pulse Profile')
xlabel('t (s)'), ylabel('I (MA)')
hold on

%discharge acceleration
figure(4)
gcf = plot(t_discharge, (a2/1000))
title('Acceleration')
xlabel('t (s)'), ylabel('a (km/s2)')
hold on
```


7.3 APPENDIX III: ANSYS SIMULATIONS





8 REFERENCES

- [1] M Ahmed (2015), “*Design of a Rail-gun Style System to Launch Cube Satellites and Other Small Payloads into Orbit*”, Queen Mary University of London School of Engineering and Materials Science
- [2] J P W Stark *et al* (2011), *Spacecraft Systems Engineering - 4th Edition*, Wiley, pp. 247-595
- [3] J Dean (2015), “*NASA Seeks Launchers For Smallest Satellites*”, Florida Today, accessed 09/11/2015
- [4] A J Sangster (2012), *Fundamentals of Electromagnetic Levitation - Engineering Sustainability through Efficiency*, Institute of Engineering and Technology, pp. 35-40
- [5] M R Doyle *et al* (1995), “*Electromagnetic Aircraft Launch System - EMALS*”, IEEE Transactions On Magnetics, Vol. 31 No. 1, pp. 528-533
- [6] S Hundertmark *et al* (2014), “*Experiments to Increase the Used Energy With the PEGASUS Railgun*”, IEEE Transactions On Plasma Science, Vol. 42 No. 10, pp. 3180-3185
- [7] I R McNab *et al* (2008), “*Electromagnetic Launch to Space*”, Acta Physica Polonia A, Vol. 115 No. 6, pp. 1066-1068
- [8] S Hundertmark *et al* (2013), “*Payload Acceleration using a 10 MJ DES Railgun*”, IEEE Transactions on Plasma Science, Vol. 41 No. 5, pp. 1455-1459
- [9] I R McNab (2003), “*Launch to Space With an Electromagnetic Railgun*”, IEEE Transactions On Magnetics, Vol. 39 No. 1, pp. 295-304
- [10] I R McNab (2007), “*A Research Program to Study Airborne Launch to Space*”, IEEE Transactions On Magnetics, Vol. 43 No.1, pp. 486-490
- [11] I R McNab (1999), “*The STAR Railgun Concept*”, IEEE Transactions On Magnetics, Vol. 35 No.1, pp. 432-436
- [12] E M Drobyshevski *et al* (2001), “*Physics of Solid Armature Launch Transition into Arc Model*”, IEEE Transactions On Magnetics, Vol. 37 No. 11, pp. 62-66
- [13] I R McNab (2009), “*Progress on Hypervelocity Railgun Research for Launch to Space*”, IEEE Transactions On Magnetics, Vol. 45 No. 1, pp. 381-388
- [14] D J Griffiths (2009), *Introduction to Electrodynamics*, Prentice Hall, pp. 215-219
- [15] Hyper-velocity Watermelon Destruction Kit (2016), “*Hyper-velocity Watermelon Destruction Kit*”, available <http://web.mit.edu/mouser/www/railgun/physics.html> accessed 06/05/2016
- [16] A S Feliciano (2001), “*The Design and Optimisation of a Power Supply for a One-Meter Electromagnetic Railgun*” - *Master's Thesis*, Naval Postgraduate School, Monterey, California
- [17] P Novak (2014), *DEN5109 - Engineering Instrumentation, Introduction to AC*, Queen Mary University of London, School of Engineering and Materials Science
- [18] I R McNab *et al* (2008), “*Megampere Pulsed Alternators for Large EM Launchers*”, IEEE International Conference on Megagauss Magnetic Field Generation and Related Topics, pp. 391-397